products). Rotation of the $NH(HgCH_3)$ group about C6-N6 was found to be a much faster process than disproportionation. This rules out the possibility that the rotamers be interconverted only via scrambling of the ligand among the four species present at equilibrium.

Although the Hg-N bonds are all labile from the standpoint of preparative chemistry, the present work indicates that the CH_3Hg^+ groups bound to very basic sites tend to exchange slowly on the NMR time scale. Indeed, an individual ^{199}Hg signal of each CH_3Hg^+ group within a molecule or of different species is observed at room temperature. Furthermore, coupling between the N6-H proton and ^{199}Hg has also been detected.

Acknowledgment. We acknowledge the valuable contribution of the "Laboratoire Régional de RMN à haut Champ" in Montréal and thank R. Mayer and S. Bilodeau for assistance with the collection of NMR data and M. Simard for valuable discussion. The financial support of the Natural Science and Engineering Research Council of Canada is gratefully acknowledged.

Supplementary Material Available: ^1H NMR spectra of mixtures of amino di-, mono-, and unsubstituted derivatives of 9-methyladenine (Figure 9) and 9-(methylmercuri)adenine (Figure 10) used for determining the K_1 constants (3 pages). Ordering information is given on any current masthead page.

Synthesis and Structures of Distibene (RSb=SbR) and Bridging Stibinidene (RSb) Iron Complexes

A. H. Cowley,*[1a] N. C. Norman,[1a] M. Pakulski,[1a] D. L. Bricker,[1b] and D. H. Russell[1b]

Contribution from the Departments of Chemistry, The University of Texas at Austin, Austin, Texas 78712, and Texas A&M University, College Station, Texas 77843.
Received May 30, 1985

Abstract: The reaction of $(Me_3Si)_2CHSbCl_2$ (**4**) with $Na_2[Fe(CO)_4]$ affords a mixture of the distibene complex, $[Fe(\eta^2\text{-}\{(Me_3Si)_2CH\}_2Sb_2)(CO)_4]$ (**5**), and the "closed" stibinidene complex, $[Fe_2\{\mu\text{-}SbCH(SiMe_3)_2\}(CO)_8]$ (**6**). The structures of **4**, **5**, and **6** were determined by single-crystal X-ray diffraction methods. Compound **4** crystallizes in the monoclinic space group $P2_1/n$ with a = 7.021 (3) Å, b = 17.129 (10) Å, c = 12.490 (4) Å, and β = 99.64 (3)°. Compound **5** crystallizes in the monoclinic space group $P2_1/n$ with a = 19.958 (4) Å, b = 6.635 (1) Å, c = 24.408 (6) Å, and β = 103.51 (2)°. Compound **6** crystallizes in the triclinic space group $P\bar{1}$ with a = 7.065 (5) Å, b = 9.179 (2) Å, c = 19.814 (7) Å, α = 86.86 (3)°, β = 85.23 (5)°, γ = 70.04 (4)°. The reaction of **5** with $Fe_2(CO)_9$ produces **6**, an unstable compound, **14**, believed to be the "open" isomer of **6**, and an iron-antimony cluster, $[\{Fe(CO)_3\}_3\{(Me_3Si)_2CHSb\}_2]$, (**15**).

The synthesis of stable compounds featuring unsupported double bonds between the heavier main-group elements has been achieved recently by use of bulky ligands.[2] With particular reference to group 5A, this strategy has proved successful for the isolation of diphosphenes (RP=PR), diarsenes (RAs=AsR), phosphaarsenes (RP=AsR), and a phosphastibene (RP=SbR). In each case the molecule contains a double bond and a lone pair of electrons on each group 5A atom. The availability of these new ligands has enabled an extensive coordination chemistry to be developed. Thus, far, a total of six different bonding modes have been recognized for RE=ER ligands.[2d,e,3] Of particular concern to the present work are the modes which feature donation by the lone pair(s) of the main-group atom, E, thus leaving an unsupported E=E bond.[3-7] The first compound of this type (**1**) was prepared by Power et al.[5] by treatment of $(Me_3Si)_2CHPCl_2$ with $Na_2[Fe(CO)_4]$. Not only does **1** possess an unsupported P=P double

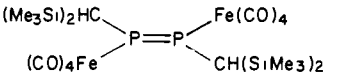

1

bond but it also features considerable steric loading at each phosphorus on account of the attachment of two $Fe(CO)_4$ moieties. Since all our attempts to prepare and isolate an unligated distibene (RSb=SbR) had met with failure, we turned our attention to the possibility of synthesizing an antimony-antimony double-bonded compound analogous to **1** using the methodology of Power et al.[5] While this objective was not realized, the work has resulted in a π-bonded distibene complex, a novel "closed" stibinidene (RSb) complex, and a cluster with an Fe_3Sb_2 core.

Results and Discussion

Our initial approach to the synthesis of compounds featuring antimony-antimony double bonds centered around the reaction of dichlorostibines with transition metal dianions. Experience gained with diphosphenes and their heavier congeners indicates that the nature of the products depended critically on the steric demands of the substituents. Since the three most widely used substituents are 2,4,6-$(t\text{-}Bu)_3C_6H_2$, $(Me_3Si)_3C$, and $(Me_3Si)_2CH$, our first objective was to prepare dichlorostibines bearing these

(1) (a) The University of Texas at Austin. (b) Texas A&M University.
(2) For reviews of group 4A compounds see: (a) West, R. *Pure Appl. Chem.* **1984**, *56*, 163. (b) West, R. In "Organosilicon and Bioorganosilicon Chemistry",; Sakurai, H., Ed.; Ellis Horwood Publishers: New York 1985. For reviews of group 5A compounds, see: (c) Cowley, A. H. *Polyhedron* **1984**, *3*, 389. (d) Cowley, A. H. *Acc. Chem. Res.* **1984**, *17*, 386. (e) Cowley, A. H.; Norman, N. C. *Prog. Inorg. Chem.*, in press.
(3) Cowley, A. H.; Kilduff, J. E.; Lasch, J. G.; Norman, N. C.; Pakulski, M.; Ando, F.; Wright, T. C. *Organometallics* **1984**, *3*, 1044 and references therein.
(4) Flynn, K. M.; Hope, H.; Murray, B.; Olmstead, M. M. *J. Am. Chem. Soc.* **1983**, *105*, 7750.
(5) Flynn, K. M.; Olmstead, M. M.; Power, P. P. *J. Am. Chem. Soc.* **1983**, *105*, 2085.
(6) Flynn, K. M.; Murray, B. D.; Olmstead, M. M.; Power, P. P. *J. Am. Chem. Soc.* **1983**, *105*, 7460.
(7) Borm, J.; Zsolnai, L.; Huttner, G. *Angew. Chem.* **1983**, *95*, 1018; *Angew. Chem., Int. Ed. Engl.* **1983**, *22*, 977.

0002-7863/85/1507-8211$01.50/0

Table I. Bond Lengths (Å) for $(Me_3Si)_2CHSbCl_2$ (**4**)[a]

atom 1	atom 2	distance	atom 1	atom 2	distance	atom 1	atom 2	distance
Sb1	Cl1	2.375 (1)	Si1	C11	1.860 (5)	Si2	C21	1.927 (7)
Sb1	Cl2	2.358 (2)	Si1	C12	1.894 (6)	Si2	C22	1.905 (6)
Sb1	C1	2.136 (4)	Si1	C13	1.898 (6)	Si2	C23	1.881 (7)
Si1	C1	1.921 (4)	Si2	C1	1.882 (4)			

[a] Numbers in parentheses are estimated standard deviations in the least significant digits.

Table II. Bond Angles (deg) for $(Me_3Si)_2CHSbCl_2$ (**4**)[a]

atom 1	atom 2	atom 3	angle	atom 1	atom 2	atom 3	angle	atom 1	atom 2	atom 3	angle
Cl1	Sb1	Cl2	93.94 (7)	C11	Si1	C12	106.5 (3)	C21	Si2	C22	103.5 (3)
Cl1	Sb1	C1	102.8 (1)	C11	Si1	C13	112.2 (3)	C21	Si2	C23	109.4 (4)
Cl2	Sb1	C1	97.7 (1)	C12	Si1	C13	104.9 (4)	C22	Si2	C23	112.2 (3)
C1	Si1	C11	113.4 (2)	C1	Si2	C21	109.9 (3)	Sb1	C1	Si1	108.5 (2)
C1	Si1	C12	110.9 (2)	C1	Si2	C22	108.6 (2)	Sb1	C1	Si2	119.8 (2)
C1	Si1	C13	108.7 (2)	C1	Si2	C23	112.9 (3)	Si1	C1	Si2	116.0 (2)

[a] Numbers in parentheses are estimated standard deviations in the least significant digits.

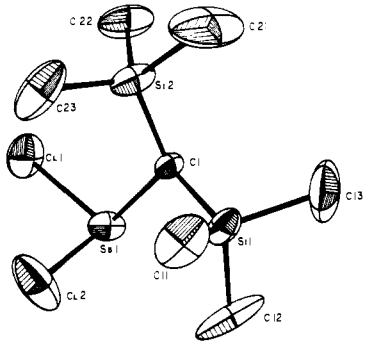

Figure 1. ORTEP view of $(Me_3Si)_2CHSbCl_2$ (**4**) showing the atom numbering scheme.

moieties. However, the attempted synthesis of (2,4,6-(t-Bu)$_3$C$_6$H$_2$)SbCl$_2$ by treatment of (2,4,6-(t-Bu)$_3$C$_6$H$_2$)Li with $SbCl_3$ resulted in the antimony heterocycle, **2**. A similar cyclization has been observed with $AsCl_3$ and presumably results from intramolecular dehydrochlorination of the precursor dichlorostibine.[8]

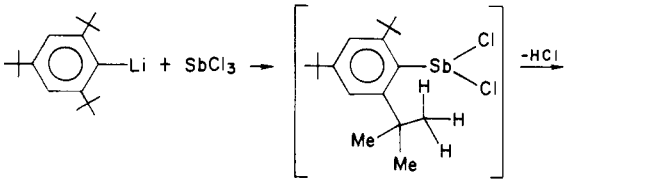

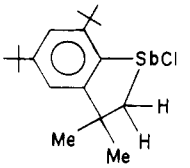

2

The reactions of $SbCl_3$ with $(Me_3Si)_3CLi$ or $(Me_3Si)_2CHMgCl$, on the other hand, proceeded in an uncomplicated fashion and resulted in the dichlorostibines **3** and **4**.[9,10] Unfortunately, however, the usefulness of **3** is complicated by its extreme sensitivity to light. As a consequence, **4** became the reagent of choice.

$(Me_3Si)_3CSbCl_2$ **3** $(Me_3Si)_2CHSbCl_2$ **4**

Table III. Atomic Coordinates for $(Me_3Si)_2CHSbCl_2$ (**4**)[a]

atom	x	y	z	B (Å^2)
Sb1	0.1976 (2)	0.11010 (6)	0.05130 (7)	3.43 (2)
Cl1	−0.2497 (7)	0.0265 (2)	−0.0713 (4)	5.6 (1)
Cl2	0.5153 (6)	0.1425 (3)	0.1329 (5)	7.6 (1)
Si1	0.1045 (6)	0.2461 (2)	0.2217 (3)	3.21 (8)
Si2	0.0757 (7)	0.0687 (2)	0.3039 (3)	3.90 (9)
C1	0.058 (2)	0.1380 (7)	0.1857 (9)	2.3 (2)
C11	0.314 (3)	0.2619 (9)	0.332 (1)	5.1 (4)
C12	0.157 (4)	0.3030 (9)	0.100 (1)	8.1 (6)
C13	−0.126 (3)	0.291 (1)	0.255 (2)	7.6 (5)
C21	−0.042 (4)	0.115 (1)	0.418 (1)	9.7 (6)
C22	−0.083 (3)	−0.0197 (9)	0.260 (1)	5.9 (4)
C23	0.332 (3)	0.040 (1)	0.360 (2)	6.9 (5)

[a] Anisotropically refined atoms are given in the form of the isotropic equivalent thermal parameter defined as $^4/_3[a^2B(1,1) + b^2B(2,2) + c^2B(3,3) + ab(\cos\gamma)B(1,2) + ac(\cos\beta)B(1,3) + bc(\cos\alpha)B(2,3)]$.

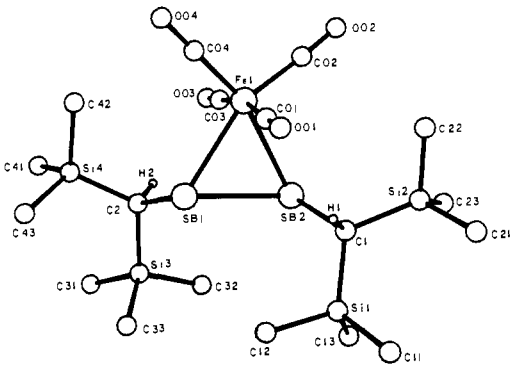

Figure 2. ORTEP view of $[Fe(\eta^2\text{-}\{(Me_3Si)_2CH\}_2Sb_2(CO)_4]$ (**5**) showing the atom numbering scheme.

The details of the synthesis of **4** have been described previously.[10] X-ray quality crystals were grown from n-hexane solutions held at −20 °C. The structure of **4** is illustrated in Figure 1 together with the atom numbering scheme. Listings of bond distances, bond angles, and atomic positional parameters are presented in Tables I–III, while pertinent crystallographic data are assembled in Table IV. The geometry around the antimony is strongly pyramidal as revealed in the three angles, Cl(1)–Sb(1)–Cl(2) = 93.94 (7)°, Cl(1)–Sb(1)–C(1) = 102.8 (1)°, and Cl(2)–Sb(1)–C(1) = 97.7 (1)°. The fact that the sum of bond angles for **4** (294.4 (1)°) exceeds that for $SbCl_3$ (285.6°)[11] is presumably a reflection of the steric demands of the $(Me_3Si)_2CH$ group. The average Sb–Cl bond length (2.366 (2) Å) and the Sb–C bond length (2.136 (4) Å) are close to the sums of single bond covalent radii (2.39 and 2.17 Å for Sb–Cl and Sb–C, respectively).[12]

(8) Cowley, A. H.; Lasch, J. G.; Norman, N. C.; Pakulski, M. *J. Am. Chem. Soc.* **1983**, *105*, 5506. Cowley, A. H.; Kilduff, J. E.; Lasch, J. G.; Mehrotra, S. K.; Norman, N. C.; Pakulski, M.; Whittlesey, B. R.; Atwood, J. L.; Hunter, W. E. *Inorg. Chem.* **1984**, *23*, 2582.

(9) Cowley, A. H.; Lasch, J. G.; Norman, N. C.; Pakulski, M.; Whittlesey, B. R. *J. Chem. Soc., Chem. Commun.* **1983**, 881.

(10) Breunig, H. J.; Kanig, W.; Soltani-Neshan, A. *Polyhedron* **1983**, *2*, 291.

(11) Lindqvist, I.; Niggli, A. *J. Inorg. Nucl. Chem.* **1956**, *2*, 345.

Table IV. Crystallographic and Intensity Data Collection Parameters for 4, 5, and 6

	4	5	6
formula	$C_7H_{19}Cl_2SbSi_2$	$C_{18}H_{38}FeO_4Sb_2Si_4$	$C_{15}H_{19}Fe_2O_8SbSi_2$
fw	352.06	730.18	616.92
crystal class	monoclinic	monoclinic	triclinic
space group	$P2_1/n$	$P2_1/n$	$P\bar{1}$
a, Å	7.021 (3)	19.958 (4)	7.065 (5)
b, Å	17.129 (10)	6.635 (1)	9.179 (2)
c, Å	12.490 (4)	24.408 (6)	19.814 (7)
α, deg			86.86 (3)
β, deg	99.64 (3)	103.51 (2)	85.23 (5)
γ, deg			70.04 (4)
U, Å^3	1481 (2)	3143 (3)	1203 (2)
Z	4	4	2
p(calcd), g cm^{-3}	1.829	1.543	1.702
radiations	graphite-monochromated Mo radiation $\lambda = 0.71069$ Å		
μ(Mo Kα), cm^{-1}	22.1	23.5	24.4
hours of data collection	33.4	74.3	57.4
% decay of standards	2.8	7.1	23.2
2θ range, deg	$2.0 \leq 2\theta \leq 50.0$		
reflcts measd	2478	5844	3859
reflcts obsd	2145	3884	3283
data omission factor	$I > 3.0\sigma(I)$		
R^a	0.0663	0.036	0.0314
Rw^b	0.0876	0.060	0.0394
no. of variables	109	262	311
GOF^c		1.555	1.448
P^d	0.06	0.08	0.04

^{a} $R = \Sigma(|F_o| - |F_c|)/\Sigma|F_o|^2$. ^{b} $Rw = [\Sigma w(|F_o| - |F_c|)^2/\Sigma|F_o|^2]^{1/2}$. ^{c} GOF $= [\Sigma w(|F_o| - |F_c|)^2/(NO - NV)]^{1/2}$. ^{d} The weighting scheme used was of the form $w = 4F_o^2/\sigma^2(F_o)^2$ and $\sigma^2(F_o^2) = \sigma_o^2(F_o^2) + (pF^2)^2$. P is an empirical factor used to downweight intense reflections. NO = no. of observed data. NV = no. of parameters varied.

The reaction of **4** with $Na_2[Fe(CO)_4]$ resulted in two products, **5** (orange) and **6** (red) which were separable by column chromatography. In each instance crystals suitable for X-ray diffraction experiments were obtained.

$(Me_3Si)_2CHSbCl_2$ + $Fe(CO)_4^{2-}$ ⟶

4

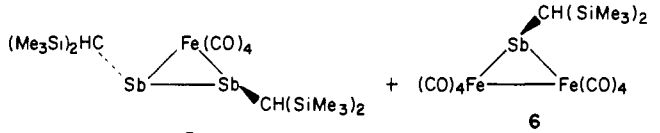

5 **6**

The structure of **5** is depicted in Figure 2 along with the atom numbering scheme adopted. This compound may be viewed as a distibene π complex in which the $(Me_3Si)_2CHSb{=}SbCH(SiMe_3)_2$ is η^2-coordinated to a $Fe(CO)_4$ moiety in a fashion analogous to the ethylene complex, $[Fe(CO)_4(\eta^2\text{-}C_2H_4)]$,[13] and the known diphosphene[4,7,14] and diarsene[15] π complexes. The antimony–antimony distance (2.774 (1) Å) is consistent with a modicum of multiplicity in this bond, being somewhat shorter than a typical Sb–Sb single bond (e.g., Ph_4Sb_2, 2.837 (1) Å).[16] Interestingly, the Sb–Sb bond length for **5** is longer than that for **7** (2.663 Å),[17] the only other structurally characterized distibene

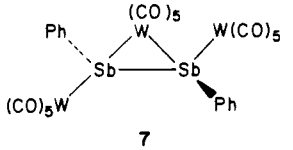

7

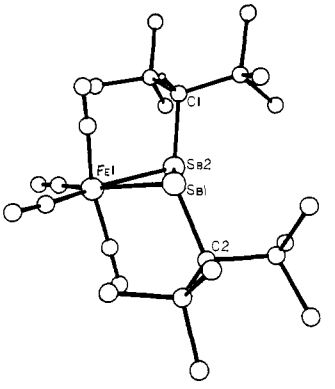

Figure 3. View of $[Fe(\eta^2\text{-}\{(Me_3Si)_2CH\}_2Sb_2)(CO)_4]$ (**5**) down the Sb(1)–Sb(2) bond.

complex. While the geometric parameters associated with the two $(Me_3Si)_2CH$ groups are unexceptional, their spatial interrelationships are worthy of comment. Note that the $(Me_3Si)_2CH$ groups adopt a mutually trans disposition with respect to the Sb–Sb vector, a feature that **5** shares in common with most other RE=ER complexes.[2d,e] The view of **5** which is presented in Figure 3 illustrates this geometry and in addition shows a bending back of these groups away from the $Fe(CO)_4$ moiety. The degree to which this bending occurs is apparent from the torsion angle of −153.0° for C(2)–Sb(1)–Sb(2)–C(1). This angle would presumably be 180° for the uncomplexed distibene $(Me_3Si)_2CHSb{=}SbCH(SiMe_3)_2$. This feature is commonly found for olefin complexes and is thus consistent with a π-complex description for **5**. Also noteworthy is the fact that each $(Me_3Si)_2CH$ group adopts a conformation which places the unique hydrogen atoms, H(1) and H(2), pointing toward the $Fe(CO)_4$ moiety. This conformation probably results from the minimization of steric congestion. The geometry around the iron atom can be viewed as being trigonal bipyramidal with the distibene occupying a single equatorial site. Equatorial coordination of the distibene

(12) Pauling, L. "The Nature of the Chemical Bond", 3rd ed.; Cornell University Press: Ithaca, NY, 1960.
(13) Davis, M. I.; Speed, C. S. *J. Organomet. Chem.*, **1970**, *21*, 401.
(14) (a) Green, J. C.; Green, M. L. H.; Morris, G. E. *J. Chem. Soc., Chem. Commun.* **1974**, 212. (b) Elmes, P. S.; Scudder, M. L.; West, B. O. *J. Organomet. Chem.* **1976**, *122*, 281. (c) Chatt, J.; Hitchcock, P. B.; Pidcock, A.; Warrens, C. P.; Dixon, K. R. *J. Chem. Soc., Dalton Trans.* **1984**, 2237.
(15) (a) Huttner, G.; Schmid, H.-G.; Frank, A.; Orama, O. *Angew. Chem.*, **1976**, *88*, 255; *Angew Chem., Int. Ed. Engl.* **1976**, *15*, 234. (b) Elmes, P. S.; Laverett, P.; West, B. O. *J. Chem. Soc., Chem. Commun.* **1971**, 747.
(16) van Deuter, K.; Rehder, D. *Cryst. Struct. Commun.* **1980**, *9*, 167.
(17) Huttner, G.; Weber, U.; Sigwarth, B.; Scheidsteger, O. *Angew. Chem., Int. Ed. Engl.* **1982**, *21*, 215.

Table V. Bond Lengths (Å) for $[Fe(\eta^2\text{-}\{(Me_3Si)_2CH\}_2Sb_2)(CO)_4]$ (**5**)[a]

atom 1	atom 2	distance	atom 1	atom 2	distance	atom 1	atom 2	distance
Sb1	Sb2	2.774 (1)	Si1	C11	1.879 (8)	Si3	C33	1.880 (8)
Sb1	Fe1	2.719 (1)	Si1	C12	1.852 (11)	Si4	C2	1.886 (6)
Sb1	C2	2.229 (5)	Si1	C13	1.878 (11)	Si4	C41	1.904 (8)
Sb2	Fe1	2.711 (1)	Si2	C1	1.883 (6)	Si4	C42	1.887 (8)
Sb2	C1	2.192 (6)	Si2	C21	1.861 (12)	Si4	C43	1.907 (9)
Fe1	C01	1.822 (8)	Si2	C22	1.834 (14)	O01	C01	1.112 (8)
Fe1	C02	1.797 (8)	Si2	C23	2.00 (2)	O02	C02	1.122 (8)
Fe1	C03	1.789 (7)	Si3	C2	1.899 (5)	O03	C03	1.163 (8)
Fe1	C04	1.795 (9)	Si3	C31	1.882 (8)	O04	C04	1.143 (10)
Si1	C1	1.897 (7)	Si3	C32	1.836 (8)			

[a] Numbers in parentheses are estimated standard deviations in the least significant digits.

Table VI. Bond Angles (deg) for $[Fe(\eta^2\text{-}\{(Me_3Si)_2CH\}_2Sb_2)(CO)_4]$ (**5**)[a]

atom 1	atom 2	atom 3	angle	atom 1	atom 2	atom 3	angle
Sb2	Sb1	Fe1	59.13 (2)	C1	Si2	C22	113.2 (5)
Sb2	Sb1	C2	101.9 (1)	C1	Si2	C23	106.8 (5)
Fe1	Sb1	C2	107.5 (1)	C21	Si2	C22	118.1 (8)
Sb1	Sb2	Fe1	59.42 (2)	C21	Si2	C23	98.1 (9)
Sb1	Sb2	C1	102.9 (2)	C22	Si2	C23	104 (1)
Fe1	Sb2	C1	107.4 (2)	C2	Si3	C31	111.1 (3)
Sb1	Fe1	Sb2	61.46 (2)	C2	Si3	C32	109.0 (3)
Sb1	Fe1	C01	81.7 (2)	C2	Si3	C33	113.0 (3)
Sb1	Fe1	C02	159.3 (3)	C31	Si3	C32	105.6 (4)
Sb1	Fe1	C03	85.9 (2)	C31	Si3	C33	106.1 (4)
Sb1	Fe1	C04	99.6 (3)	C32	Si3	C33	111.8 (4)
Sb2	Fe1	C01	87.2 (2)	C2	Si4	C41	110.0 (3)
Sb2	Fe1	C02	97.8 (3)	C2	Si4	C42	111.6 (3)
Sb2	Fe1	C03	83.6 (2)	C2	Si4	C43	110.5 (3)
Sb2	Fe1	C04	161.0 (3)	C41	Si4	C42	106.5 (4)
C01	Fe1	C02	97.5 (3)	C41	Si4	C43	110.3 (4)
C01	Fe1	C03	167.1 (3)	C42	Si4	C43	108.0 (5)
C01	Fe1	C04	90.2 (3)	Fe1	C01	O01	177.7 (6)
C02	Fe1	C03	92.8 (3)	Fe1	C02	O02	177.8 (9)
C02	Fe1	C04	101.1 (4)	Fe1	C03	O03	177.3 (6)
C03	Fe1	C04	95.6 (3)	Fe1	C04	O04	174.2 (8)
C1	Si1	C11	113.5 (4)	Sb2	C1	Si1	109.5 (3)
C1	Si1	C12	108.9 (4)	Sb2	C1	Si2	110.4 (3)
C1	Si1	C13	112.0 (5)	Si1	C1	Si2	117.5 (3)
C11	Si1	C12	102.1 (5)	Sb1	C2	Si3	108.4 (3)
C11	Si1	C13	109.3 (6)	Sb1	C2	Si4	107.9 (3)
C12	Si1	C13	110.6 (8)	Si3	C2	Si4	116.9 (3)
C1	Si2	C21	113.9 (4)				

[a] Numbers in parentheses are estimated standard deviations in the least significant digits.

ligand is favored on steric grounds, and this site preference has been observed previously for $Fe(CO)_4$ complexes of diphosphene and diarsene ligands. The listings of bond lengths, interbond angles, and atomic positional parameters for **5** are assembled in Tables V–VII.

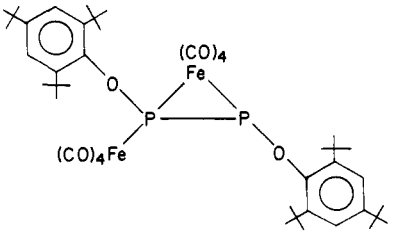

8[4]

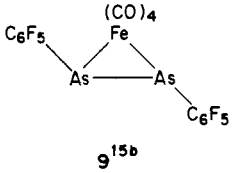

9[15b]

As shown in Figure 4, the structure of **6** comprises a Fe_2Sb three-membered ring and can be discussed as a diiron complex containing a bridging stibinidene unit. The molecule as a whole possesses near mirror symmetry with the plane defined by C(1), Sb(1), and the Fe(1), Fe(2) midpoint. The Me_3Si groups, however, deviate from this ideal since the methyl groups are approximately staggered. Each iron adopts a distorted octahedral geometry, being bonded to four terminal carbonyls, the antimony, and another iron atom. The iron–iron separation (2.801 (1) Å) is somewhat long but is consistent with a single bond formulation. The antimony atom adopts a pyramidal geometry and can be

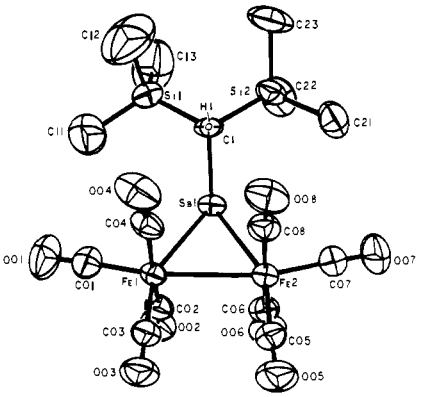

Figure 4. ORTEP view of $[Fe_2\{\mu\text{-}SbCH(SiMe_3)_2\}(CO)_8]$ (**6**) showing the atom numbering scheme.

regarded as being singly bonded to Fe(1) (2.633 (1) Å), Fe(2) (2.641 (1) Å), and C(1) (2.208 (5) Å). The fact that the sum of angles at Sb is less for **6** (287.1°) than that for **4** (294.4°) presumably results from incorporation into a cyclic unit. Listings of bond lengths, interbond angles, and atomic positional parameters for **6** are given in Tables VIII–X while pertinent crystallographic data for both **5** and **6** are collected in Table IV.

Attention is now turned to the qualitative bonding descriptions for **5** and **6**. The bonding in **5** can be discussed in terms of two canonical forms, **5a** and **5b**. Form **5a** represents a π-complex

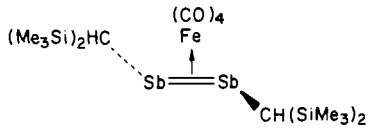

5a

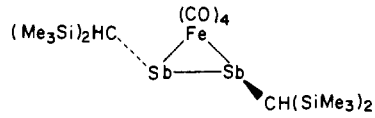

5b

formalism as previously discussed in this section. Form **5b**, on the other hand, may be described as a metallacyclic structure involving σ bonding between the three central atoms. This latter description can also be used to represent the bonding in **6** if it is considered as a dimetallastibine. The description of **5** and **6** as

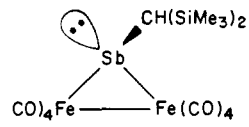

6

metallacycles is useful because it serves to illustrate isolobal relationships.[18] For example, the $Fe(CO)_4$ and RSb units are isolobal and therefore, to a first approximation, interchangable. Compounds **5** and **6** can now be seen as the two intermediate members of a more extensive series of molecules shown below.

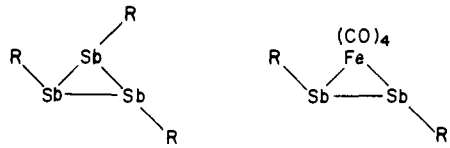

10

5

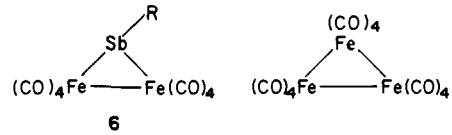

6

The cyclotristibine (**10**), where R = $(Me_3Si)_2CH$, is a known compound although it has not been structurally characterized.[19] Triiron dodecacarbonyl is represented here as a simple trimer of $Fe(CO)_4$ units, even though the observed structure features two bridging carbonyls.[20] Nevertheless, the point has been made that such bridging groups do not, to a first approximation, affect the nature of the frontier orbitals on which the isolobal principle is based; moreover, the heavier congeneric compounds $Ru_3(CO)_{12}$ and $Os_3(CO)_{12}$ adopt the structure with all terminal carbonyls.[20] A further extension of structural relationships becomes apparent when it is recognized that the $Fe(CO)_4$ and RSb moieties are isolobal with a methylene group. Structures **5**, **6**, and **10** may then be considered as cyclopropane analogues. A further novel aspect of **6** concerns the fact that it adopts a "closed" structure, i.e., the stibinidene moiety bridges an Fe–Fe bond and adopts a pyramidal geometry. Compound **6** represents the first example of such a complex since all other "inidene" systems are "open" as shown in **11**,[6,21] containing a trigonal planar E atom and no M–M bond. (It should, however, be noted that derivatives of a "closed"-type compound like **6** are known where the E lone pair is coordinated to another ML_n fragment.[22]) It is apparent that

Table VII. Atomic Coordinates for $[Fe(\eta^2\text{-}\{(Me_3Si)_2CH\}_2Sb_2)(CO)_4]$ (**5**)

atom	*x*	*y*	*z*	*B* (Å^2)
Sb1	0.46351 (3)	0.26034 (9)	0.18332 (2)	3.77 (1)
Sb2	0.51786 (3)	−0.02189 (9)	0.26558 (2)	3.90 (1)
Fe1	0.59491 (6)	0.1248 (2)	0.19670 (6)	4.42 (3)
Si1	0.4592 (2)	0.2036 (5)	0.3677 (1)	5.67 (7)
Si2	0.6171 (2)	0.0494 (6)	0.3952 (1)	6.84 (9)
Si3	0.3130 (1)	0.0173 (4)	0.1401 (1)	4.51 (6)
Si4	0.3884 (2)	0.1974 (5)	0.0473 (1)	5.15 (6)
O01	0.6249 (4)	0.477 (1)	0.2709 (4)	7.8 (2)
O02	0.7212 (4)	−0.101 (2)	0.2422 (5)	10.6 (3)
O03	0.5365 (4)	−0.217 (1)	0.1239 (3)	7.0 (2)
O04	0.6379 (4)	0.369 (2)	0.1107 (4)	10.0 (2)
C01	0.6127 (4)	0.342 (2)	0.2435 (4)	5.4 (2)
C02	0.6727 (5)	−0.013 (2)	0.2257 (5)	6.5 (3)
C03	0.5579 (5)	−0.080 (2)	0.1523 (4)	5.2 (2)
C04	0.6200 (6)	0.267 (2)	0.1421 (5)	7.3 (3)
C1	0.5413 (5)	0.159 (2)	0.3429 (4)	4.8 (2)
C2	0.3963 (4)	0.070 (1)	0.1176 (3)	3.7 (2)
C11	0.4738 (8)	0.338 (2)	0.4372 (5)	9.9 (4)
C12	0.4045 (7)	0.385 (3)	0.3194 (6)	12.1 (4)
C13	0.4110 (9)	−0.037 (3)	0.3716 (7)	14.0 (5)
C21	0.6320 (7)	0.164 (2)	0.4667 (6)	13.7 (4)
C22	0.6920 (7)	0.004 (2)	0.3654 (6)	15.1 (4)
C23	0.5891 (8)	−0.226 (2)	0.4148 (6)	15.6 (4)
C31	0.2447 (5)	−0.083 (2)	0.0795 (5)	7.3 (3)
C32	0.3283 (5)	−0.184 (2)	0.1932 (4)	6.8 (3)
C33	0.2755 (6)	0.249 (2)	0.1657 (5)	8.1 (3)
C41	0.3461 (6)	0.020 (2)	−0.0120 (4)	7.2 (3)
C42	0.4756 (6)	0.264 (2)	0.0348 (5)	8.1 (3)
C43	0.3363 (8)	0.440 (2)	0.0437 (5)	8.7 (4)

Table VIII. Bond Lengths (Å) for $[Fe_2\{\mu\text{-}SbCH(SiMe_3)_2\}(CO)_8]$ (**6**)[a]

atom 1	atom 2	distance	atom 1	atom 2	distance
Sb1	Fe1	2.633 (1)	Si1	C13	1.902 (11)
Sb1	Fe2	2.641 (1)	Si1	C11A	2.00 (2)
Sb1	C1	2.208 (5)	Si1	C12A	1.81 (3)
Fe1	Fe2	2.801 (1)	Si1	C13A	1.87 (3)
Fe1	C01	1.780 (5)	Si2	C1	1.887 (4)
Fe1	C02	1.809 (5)	Si2	C21	1.844 (6)
Fe1	C03	1.808 (4)	Si2	C22	1.856 (7)
Fe1	C04	1.781 (5)	Si2	C23	1.853 (9)
Fe2	C05	1.811 (6)	O01	C01	1.146 (6)
Fe2	C06	1.814 (5)	O02	C02	1.147 (7)
Fe2	C07	1.779 (5)	O03	C03	1.145 (6)
Fe2	C08	1.802 (6)	O04	C04	1.135 (7)
Si1	C1	1.894 (4)	O05	C05	1.139 (7)
Si1	C11	1.878 (8)	O06	C06	1.136 (6)
Si1	C12	1.878 (13)	O07	C07	1.142 (6)
			O08	C08	1.142 (7)

[a] Numbers in parentheses are estimated standard deviations in the least significant digits.

(18) Elian, M.; Chen, M. M. L.; Mingos, D. M. P.; Hoffmann, R. *Inorg. Chem.* **1976**, *15*, 1148. Hoffmann, R. *Angew. Chem., Int. Ed. Engl.* **1982**, *21*, 711. Stone, F. G. A. *Ibid.* **1984**, *23*, 89.

(19) Breunig, H. J.; Sontani-Neshan, A. *J. Organomet. Chem.* **1984**, *262*, C27.

(20) Cotton, F. A.; Wilkinson, G. "Advanced Inorganic Chemistry", 4th ed.; Wiley-Interscience: New York, 1980.

(21) RP complexes: Huttner, G.; Müller, H. D.; Frank, A.; Lorenz, H. *Angew. Chem., Int. Ed. Engl.* **1975**, *14*, 705. Huttner, G.; Borm, J.; Zsolnai, L. *J. Organomet. Chem.* **1984**, *263*, C33. Schneider, J.; Zsolnai, L.; Huttner, G. *Chem. Ber.* **1982**, *115*, 989. Lang, H.; Zsolnai, L.; Huttner, G. *Angew. Chem., Int. Ed. Engl.* **1983**, *22*, 976. Lang. H.; Mohr, G.; Scheidsteger, O.; Huttner, G. *Chem. Ber.* **1985**, *118*, 574. RAs complexes: von Seyerl, J.; Moering, U.; Wagner, A.; Frank, A.; Huttner, G. *Angew. Chem., Int. Ed. Engl.* **1978**, *17*, 844. Huttner, G.; Schmid, H.-G. *Angew. Chem., Int. Ed. Engl.* **1975**, *14*, 433. Huttner, G.; von Seyerl, J.; Marsili, M.; Schmid, H.-G. *Angew. Chem., Int. Ed. Engl.* **1975**, *14*, 434. von Seyerl, J.; Huttner, G. *Angew. Chem., Int. Ed. Engl.* **1979**, *18*, 233. Sigwarth, B.; Zsolnai, L.; Scheidsteger, O.; Huttner, G. *J. Organomet. Chem.* **1982**, *235*, 43. von Seyerl, J.; Sigwarth, B.; Schmid, H.-G.; Mohr, G.; Frank, A.; Marsili, M.; Huttner, G. *Chem. Ber.*, **1981**, *114*, 1392. Jones, R. A.; Whittlesey, B. R. *Organometallics* **1984**, *3*, 469. von Seyerl, J.; Sigwarth, B.; Huttner, G. *Chem. Ber.* **1981**, *114*, 1407. von Seyerl, J.; Sigwarth, B.; Huttner, G. *Chem. Ber.*, **1981**, *114*, 727. RSb complexes: von Seyerl, J.; Huttner, G. *Angew. Chem., Int. Ed. Engl.* **1978**, *17*, 843. Weber, U.; Zsolnai, L.; Huttner, G. *J. Organomet. Chem.* **1984**, *260*, 281. RBi complexes: von Seyerl, J.; Huttner, G. *J. Organomet. Chem.* **1980**, *195*, 207.

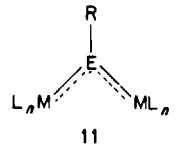

11

R = alkyl, aryl, halogen
E = P, As, Sb, Bi
ML_n = $Mn(CO)_2(\eta\text{-}C_5H_5)$, $M(CO)_5$ (M = Cr, Mo, W)

all the "open" systems feature metals from either group 6B or group 7B while **6** involves a group 8B metal. The most obvious difference between **6** and the "open" complexes concerns the coordination number of the metal. All the complexes represented by **11** would become seven-coordinate if a "closed" structure were adopted. However, the preference of an "open" or a "closed" structure probably also depends on the subtle interplay of several other factors including the tendency toward metal–metal bond formation, the nature of the ligands, and the pyramidal inversion barrier at E. Theoretical studies are in progress in an attempt to address such questions.

The bonding in species of the general type represented by **11** and **6** is interesting and deserves special comment. As previously discussed, the isolobal mapping of the fragments $Fe(CO)_4$ and RSb with CH_2 allows the analogy between **6** and cyclopropane to be drawn. The RSb group is thus behaving as a bridging methylene and adopts a pyramidal configuration with a localized nonbonding electron pair. The "open" form, represented by **11**, has been extensively studied by Huttner et al.,[21] who, together with Kostič and Fenske,[23] have proposed a delocalized 3-center 4-electron-bonding description for **11** analogous to the allyl anion in which the RE fragment is behaving as CH^- rather than as CH_2 in **6**. The relationship between **6** and **11** is now apparent if it is accepted that their analogies to cyclopropane (or more exactly the cyclopropyl anion) and the allyl anion are accurate, namely that the two are related by an electrocyclic rearrangement.[24] A more detailed theoretical treatment of their relationship is in progress.[25]

We note also that these bonding descriptions for **11** and **6** permit an understanding of their reaction chemistry. Thus Huttner et al. have observed that "open" RE complexes form adducts with, e.g., phosphines at E[21] resulting from a degree of Lewis acidity conferred by the presence of a low-lying predominantly E-centered LUMO. In contrast, a "closed" system such as **6** is anticipated to behave as a Lewis base because of the presence of a lone pair of electrons at the E atom. This expectation is supported by the observation that **6** reacts with $HBF_4 \cdot Et_2O$ to afford the marginally stable cation **12**. (Spectroscopic data for **12** are given in the Experimental Section although the thermal instability of this species precluded a more complete characterization).

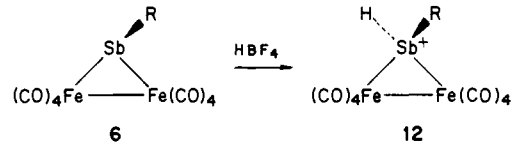

6 12

R = CH(SiMe3)2

Since compounds **5** and **6** are both formed in the reaction of **4** with $Na_2[Fe(CO)_4]$, it was of interest to establish whether **5**

Scheme I

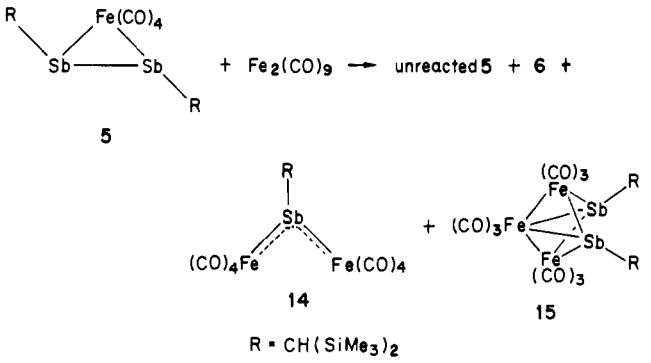

5 14 15

R = CH(SiMe3)2

could be converted into the more iron-rich compound **6** by treatment with $Fe_2(CO)_9$. This is indeed the case; however, two new compounds were also formed (Scheme I). The four compounds shown in Scheme I were separated by column chromatography (silica gel/*n*-hexane) of the crude reaction mixture. Of the two new compounds **14** and **15**, **14** is particularly interesting. Even though the column retention time of **14** is quite distinct from that of **6**, the spectroscopic properties of **14** were identical with those of **6**. Moreover, a preliminary X-ray diffraction study of crystals of **14** revealed that the unit cell dimensions were the same as those of **6** within experimental error. It is thus obvious that crystals of **6** and **14** are the same compound, i.e., **6**. Tentatively, we suggest that in solution, **14** is the "open" form of **6** (Scheme I) and that either in solution or upon crystallization it rearranges to the "closed" form, **6**. Inferentially, the energies of the "open" and "closed" forms of $[Fe_2\{\mu\text{-}SbCH(SiMe_3)_2\}(CO)_8]$ are close.

The second product, **15**, was obtained in a crystalline form. However, even thourgh an X-ray data set was collected, we were unable to solve the structure because of severe disorder problems. Preliminary spectroscopic work (IR, NMR) revealed the presence of both iron carbonyl and $(Me_3Si)_2CH$ moieties but gave no hint as to the structure. Conventional electron impact (EI) mass spectrometry yielded a peak at *m/e* 980 corresponding to $C_{23}H_{38}O_9Sb_2Fe_3Si_4$. However, since organometallic cluster compounds are often significantly fragmented during EI mass spectral assay, the compound was investigated by the relatively new technique of fast-atom bombardment (FAB) mass spectrometry. Full details of this technique are presented in the Experimental Section. The FAB mass spectrum also exhibited a signal at *m/e* 980, consistant with the above formulation. The calculated isotopic pattern for this formulation gave excellent agreement (5% error) with that observed experimentlaly. In addition, fragment ions were observed due to loss of carbonyl groups up to and including a peak at *m/e* 728 due to loss of all nine CO ligands. Collectively, these data lead to the structure assignment for **15** shown in Scheme I. Similar structures have been established by X-ray crystallography for $Fe_3(CO)_9(\mu_3\text{-}NMe)_2$[26] and $Fe_3(CO)_9(\mu_3\text{-}AsPh)_2$.[27]

Experimental Section

General Procedures. All experiments were performed under an atmosphere of dry dinitrogen by using Schlenk techniques. All solvents were freshly distilled over CaH_2 or Na/benzophenone prior to use.

Spectroscopic Measurements. Medium- and high-resolution mass spectra (HRMS) were measured on DuPont-Consolidated Model 21-491 and 21-100 instruments, respectively. Perfluorokerosene was used as the calibrant for HRMS. IR spectra were measured on a Perkin-Elmer 1330 spectrophotometer.

Starting Materials. The compounds $Na_2[Fe(CO)_4]$[28] and $(Me_3Si)_2CHSbCl_2$ (**4**)[9,10] were prepared according to literature methods. Clear, colorless single crystals of **4** suitable for X-ray crystallography were grown from *n*-hexane solution at −20 °C. All other materials were

(22) Schneider, J.; Huttner, G. *Chem. Ber.* **1983**, *116*, 917. Huttner, G.; Sigwarth, B.; von Seyerl, J.; Zsolnai, L. *Chem. Ber.* **1982**, *115*, 2035. von Seyerl, J.; Wohlfahrt, L.; Huttner, G. *Chem. Ber.* **1980**, *113*, 2868. Huttner, G.; Mohr, G.; Friedrich, P.; Schmid, H.-G. *J. Organomet. Chem.* **1978**, *160*, 59.

(23) Kostič, N. M.; Fenske, R. F. J. *Organomet. Chem.* **1982**, *233*, 337.

(24) Arif, A. M.; Cowley, A. H.; Norman, N. C.; Orpen, A. G.; Pakulski, M. *J. Chem. Soc., Chem. Commun.* **1985**, 1267.

(25) A referee has suggested that the names "phosphinidene", "arsinidene", and "stibinidene" be reserved for "open" complexes of type **11** while the term "dimetallastibine" be applied to **6**. In view of the above-mentioned relationship between these two types of complex, we prefer to use the term "stibinidene" forer both **6** and **11** since any differentiation in nomenclature would be somewhat artificial.

(26) Doedens, R. J. *Inorg. Chem.* **1969**, *8*, 570.

(27) Huttner, G.; Mohr, G.; Frank, A.; Schubert, U. *J. Organomet. Chem.* **1976**, *118*, C 73. Jacob, M.; Weiss, E. *J. Organomet. Chem.* **1977**, *131*, 263.

(28) Collman, J. P. *Acc. Chem. Res.* **1975**, *8*, 342 and references therein. See also: Collman, J. P.; Winter, S. R., U.S. Patent 3872 218 (March 18, 1975).

Table IX. Bond Angles (deg) for $[Fe_2\{\mu\text{-}SbCH(SiMe_3)_2\}(CO)_8$ (**6**)[a]

atom 1	atom 2	atom 3	angle	atom 1	atom 2	atom 3	angle
Fe1	Sb1	Fe2	64.15 (2)	C05	Fe2	C06	95.2 (3)
Fe1	Sb1	C1	110.81 (9)	C05	Fe2	C07	87.4 (3)
Fe2	Sb1	C1	112.1 (1)	C05	Fe2	C08	170.5 (2)
Sb1	Fe1	Fe2	58.06 (2)	C06	Fe2	C07	101.8 (2)
Sb1	Fe1	C01	110.1 (2)	C06	Fe2	C08	94.2 (2)
Sb1	Fe1	C02	85.1 (1)	C07	Fe2	C08	92.1 (3)
Sb1	Fe1	C03	149.5 (1)	C1	Si1	C11	116.6 (3)
Sb1	Fe1	C04	84.6 (1)	C1	Si1	C12	108.3 (4)
Fe2	Fe1	C01	168.1 (2)	C1	Si1	C13	113.4 (3)
Fe2	Fe1	C02	89.7 (1)	C1	Si1	C11A	106.7 (6)
Fe2	Fe1	C03	91.5 (1)	C1	Si1	C12A	115.0 (8)
Fe2	Fe1	C04	91.4 (1)	C1	Si1	C13A	110.0 (7)
C01	Fe1	C02	87.5 (2)	C11	Si1	C12	106.1 (5)
C01	Fe1	C03	100.4 (2)	C11	Si1	C13	105.5 (5)
C01	Fe1	C04	88.8 (2)	C12	Si1	C13	106.2 (5)
C02	Fe1	C03	97.7 (2)	C11A	Si1	C12A	106 (1)
C02	Fe1	C04	167.1 (2)	C11A	Si1	C13A	109.7 (9)
C03	Fe1	C04	95.1 (2)	C12A	Si1	C13A	110 (1)
Sb1	Fe2	Fe1	57.79 (2)	C1	Si2	C21	112.0 (2)
Sb1	Fe2	C05	85.7 (2)	C1	Si2	C22	111.5 (3)
Sb1	Fe2	C06	152.2 (1)	C1	Si2	C23	111.5 (2)
Sb1	Fe2	C07	106.0 (2)	C21	Si2	C22	107.1 (3)
Sb1	Fe2	C08	85.3 (2)	C21	Si2	C23	105.0 (3)
Fe1	Fe2	C05	89.3 (2)	C22	Si2	C23	109.5 (3)
Fe1	Fe2	C06	94.4 (1)				
Fe1	Fe2	C07	163.6 (2)				
Fe1	Fe2	C08	88.5 (1)				
Fe1	C01	O01	177.3 (5)				
Fe1	C02	O02	174.3 (4)				
Fe1	C03	O03	177.1 (4)				
Fe1	C04	O04	174.8 (4)				
Fe2	C05	O05	173.7 (4)				
Fe2	C06	O06	177.1 (4)				
Fe2	C07	O07	177.5 (5)				
Fe2	C08	O08	175.1 (4)				
Sb1	C1	Si1	110.2 (2)				
Sb1	C1	Si2	109.3 (2)				
Si1	C1	Si2	114.6 (2)				

[a] Numbers in parentheses are estimated standard deviations in the least significant digits.

procurred commercially and used as supplied.

Preparation of $[Fe(\eta^2\text{-}\{(Me_3Si)_2CH\}_2Sb_2)(CO)_4]$ (5) and $[Fe_2\{\mu\text{-}SbCH(SiMe_3)_2\}(CO)_8]$ (6). A mixture of $(Me_3Si)_2CHSbCl_2$ (4) (1.06 g, 3.0 mmol) and $Na_2[Fe(CO)_4 \cdot {}^3/_2(C_4H_8O_2)]$ (1.04 g, 3.0 mmol) in 50 mL of THF was stirred for 2 h at 25 °C. The solvent was removed in vacuo and the products were separated by column chromatography (silica gel/*n*-hexane) to afford a 20% yield of $[Fe(\eta^2\text{-}\{(Me_3Si)_2CH\}_2Sb_2)(CO)_4]$ (**5**) and a 14% yield of $[Fe_2\{\mu\text{-}SbCH(SiMe_3)_2\}(CO)_8]$ (**6**). Crystals of **5** (orange) and **6** (red) suitable for X-ray diffraction experiments were grown from *n*-hexane solutions held at −20 °C. The melting points of **5** and **6** were 111–113 and 84–86 °C, respectively. HRMS: **5**, calcd 727.9271, found 727.9246; **6**, calcd 615.8354, found 615.8333. IR (CH_2Cl_2): **5** 1995 (br) 2060 (sharp); **6**, 2005, 2020, 2040, 2090 cm^{-1}.

Reaction of $[Fe(\eta^2\{(Me_3Si)_2CH\}_2Sb_2)(CO)_4]$ (5) with $Fe_2(CO)_9$. A mixture of $[Fe(\eta^2\text{-}\{(Me_3Si)_2CH\}_2Sb_2)(CO)_4]$ (**5**) (0.22 g, 0.3 mmol) and $Fe_2(CO)_9$ (0.33 g, 0.9 mmol) in 50 mL of *n*-hexane was subjected to ultrasonic radiation at 25 °C for 1 h. After the solvent was stripped, the crude reaction mixture was separated by column chromatography (silica gel/*n*-hexane). The first fraction consisted of traces of starting material (**5**). The second fraction (32% yield based on **5**) comprised $[Fe_2\{\mu\text{-}SbCH(SiMe_3)_2\}(CO)_8]$ (**6**), and the third fraction (27% yield based on **5**) was identified as $\{Fe(CO)_3\}_3\{(Me_3Si)_2CHSb\}_2$ (**15**) by fast atom bombardment mass spectrometry (vide infra). Black crystalline **15** (mp 160–162 °C) was recrystallized from *n*-hexane solution at −20 °C. IR for **15** (CH_2Cl_2): 1985, 2020 cm^{-1}. The fourth (unstable) fraction is believed to be the "open" stibinidene complex $[Fe_2\{\mu\text{-}SbCH(SiMe_3)_2\}(CO)_8]$ (**14**). However, the spectroscopic properties of this product was identical with those of **6** in all respects.

X-ray Analysis of $(Me_3Si)_2CHSbCl_2$ (4). A suitable single crystal of dimensions 0.4 × 0.3 × 0.3 mm was sealed in a Lindemann capillary and mounted on an Enraf-Nonius CAD4-F diffractometer. Initial lattice parameters were determined from a least-squares fit to 25 accurately centered reflections, $15 \le 2\theta \le 20°$, and subsequently refined by using higher angle data. These indicated a monoclinic lattice. Data were collected for one independant quadrant, $+h+k\pm l$, using the ω–2θ scan mode. The final scan speed for each reflection was determined from the net intensity gathered during an intial prescan and ranged from 2 to 7 deg min^{-1}. The ω-scan angle was determined for each reflection according to the equation $A + B \tan\theta$ for which A and B were set at values 0.8 and 0.35, respectively. Aperture settings were derived in a like manner with A = 4.0 mm and B = 1.0 mm. Crystal stability was monitored every 30 min throughout data collection by means of two check reflections. Systematic absences observed were $0k0$ absent for k odd and $h01$ absent for $h + 1$ odd, thus uniquely determining the space group as $P2_1/n$.

Data were corrected for the effects of Lorentz, polarization, and decay but not for absorption. Merging of equivalent reflections gave a total of 2478 unique measured data for which 1329 were considered observed, $I > 3.0\sigma(I)$. The position of the antimony atoms was revealed from a Patterson map and all other non-hydrogen atoms from a subsequent difference Fourier map. All non-hydrogen atoms were refined with use of anisotropic thermal parameters. The hydrogen atoms were placed in calculated positions 0.95 Å from their respective carbon atoms and included in the structure factor calculation. In the final stages of refinement a weighting scheme was introduced to downweight intense reflections according to the form given in Table IV. Final refinement using full-matrix, least-squares converged smoothly to produce the values given in Table II. No chemically significant peaks were present in the final difference map.

X-ray Analysis of $[Fe(\eta^2\text{-}\{(Me_3Si)_2CH\}_2Sb_2)(CO)_4]$ (5) and $[Fe_2\{\mu\text{-}SbCH(SiMe_3)_2\}(CO)_8]$ (6). The details of data collection for **5** and **6** were the same as described for **4**. Both structures were solved with use direct methods (MULTAN)[29] which revealed the position of the iron and antimony atoms. Subsequent refinement was carried out as described for **4**.

Fast Atom Bombardment Mass Spectral Study of $\{[Fe(CO)_3]_3\text{-}\{(Me_3Si)_2CHSb\}_2$ (15). The mass spectrum of compound **15** was obtained by using fast-atom-bombardment (FAB) ionization on the Kratos MS-50TA at Texas A&M University. The conditions for FAB ionization were as follows: bombardment with Xe atoms with nominal energy of 8 keV (beam density of 10 μA, as measured on the Ion Tech source

(29) Main, P. MULTAN 82: University of York, York, England, 1982.

Table X. Atomic Coordinates for $[Fe_2\{\mu\text{-}SbCH(SiMe_3)_2\}(CO)_8$ (**6**)[a]

atom	x	y	z	B (Å²)
Sb1	0.18849 (4)	0.25626 (3)	0.23414 (1)	3.308 (5)
Fe1	0.46510 (8)	0.05588 (6)	0.15644 (3)	3.28 (1)
Fe2	0.26089 (9)	0.35915 (7)	0.11103 (3)	3.67 (1)
Si1	0.4018 (2)	0.1941 (2)	0.38367 (7)	5.07 (3)
Si2	0.1563 (2)	0.5406 (2)	0.33793 (7)	4.50 (3)
O01	0.6202 (7)	−0.2466 (4)	0.2258 (2)	8.4 (1)
O02	0.1358 (5)	−0.0503 (4)	0.1220 (2)	6.10 (9)
O03	0.7198 (6)	−0.0179 (5)	0.0286 (2)	6.3 (1)
O04	0.7580 (5)	0.1462 (5)	0.2236 (2)	6.9 (1)
O05	−0.0753 (5)	0.2711 (5)	0.0696 (2)	6.6 (1)
O06	0.4737 (7)	0.3261 (5)	−0.0247 (2)	7.4 (1)
O07	−0.0182 (7)	0.6765 (5)	0.0980 (3e	8.9 (1)
O08	0.5556 (5)	0.4682 (4)	0.1699 (2)	6.23 (9)
C01	0.5581 (7)	−0.1264 (5)	0.2001 (3)	5.2 (1)
C02	0.2592 (7)	−0.0021 (5)	0.1336 (2)	4.3 (1)
C03	0.6170 (7)	0.0131 (5)	0.0772 (2)	4.4 (1)
C04	0.6385 (6)	0.1180 (5)	0.1973 (2)	4.3 (1)
C05	0.0589 (7)	0.2971 (6)	0.0873 (2)	4.6 (1)
C06	0.3941 (8)	0.3347 (5)	0.0279 (2)	4.9 (1)
C07	0.0910 (9)	0.5529 (6)	0.1046 (3)	5.7 (1)
C08	0.4439 (7)	0.4201 (5)	0.1488 (2)	4.4 (1)
C1	0.3289 (6)	0.3422 (5)	0.3115 (2)	3.44 (9)
C11	0.507 (2)	−0.015 (1)	0.3600 (5)	14.8 (4)
C12	0.602 (2)	0.232 (1)	0.4292 (6)	20.5 (4)
C13	0.186 (2)	0.207 (1)	0.4497 (5)	16.1 (4)
C21	0.131 (1)	0.6868 (6)	0.2685 (3)	6.7 (2)
C22	−0.1015 (9)	0.5402 (7)	0.3647 (4)	7.4 (2)
C23	0.257 (1)	0.6135 (8)	0.4073 (4)	10.0 (2)
C11A	0.684 (3)	0.055 (2)	0.360 (1)	*****
C12A	0.409 (4)	0.273 (3)	0.465 (1)	*****
C13A	0.229 (3)	0.078 (3)	0.392 (1)	*****

[a] Asterisked atoms were refined isotropically.

control unit), ion source acceleration, potential of 8 kV, scanning the mass range m/e 1000 to m/e 50. The liquid matrix employed for the FAB ionization was commercial grade *o*-nitrophenyl octyl ether (Fluka AG, Chem.). The sample was not sufficiently soluble in glycerol or thioglycerol for FAB–MS analysis. For the mass spectral analysis, 0.1 μg of the sample was dissolved in approximately 3 μL of *o*-nitrophenyl octyl ether on the FAB direct insertion probe. The mass scale was calibrated with glycerol and/or CsI dissolved in glycerol.

The mass spectrum of **15** gave intense ions at m/e 980, 952, 896, 738, 644, 569, and 420. The signal at m/e 980 comprises a complex pattern arising from the isotopic composition $Fe_3Sb_2Si_4C_{23}H_{38}O_9$. A calculated isotopic pattern[30] for $Fe_3Sb_2Si_4C_{23}H_{38}O_9$ gave excellent agreement (5% error) with the experimentally observed isotopic pattern. The fragment ions observed and the corresponding isotopic patterns are also consistent with the proposed structure. For example, the intense ion at m/e 952 arises by loss of 28 mass units (CO) from the molecule ion. Likewise, the signals at m/e 896 and m/e 728 arise by loss of 3 and 9 carbonyl ligands, respectively. Expulsion of weakly bound ligands such as CO is common for such materials.[31] Presumably the signal at m/e 644 corresponds to loss of $Fe_2(CO)_8$, and the signal at m/e 569 corresponds to loss of $Fe_2(CO)_8$ plus Me_3Si. A series of signals beginning at m/e 420 and separated by 15 mass units correspond to successive loss of methyl groups from the $Fe_2(CO)_6SbCH(SiMe_3)_2^+$ fragment ion. This series of ions covers the mass range m/e 420–330, which corresponds to successive losses of all six methyl groups.

The proposed fragmentation patterns for **15** have been substantiated by using FAB–TMS (tandem mass sepctrometry). The specific details of these experiments on **15** and similar metal cluster ions will be presented in a separate publication.

Acknowledgment. The authors are grateful to the National Science Foundation and the Robert A. Welch Foundation for financial support.

Supplementary Material Available: Tables of thermal parameters, hydrogen atom coordinates, and observed and calculated structure factors (57 pages). Ordering information is given on any current masthead page.

(30) Yergey, J.; Heller, D.; Hansen, G.; Cotter, R. J.; Fenselan, C. *Anal. Chem.* **1983**, *55*, 353.
(31) Litzow, M. R.; Spalding, T. R. "Mass Spectrometry of Inorganic and Organometallic Compounds"; Elcevier Scientific Publishing Co.: Amsterdam-London-New York, 1973.

Base-Catalyzed Reactions of Triarylmethyl Carbocations with Water

Joseph R. Gandler

Contribution from the Department of Chemistry, California State University, Fresno, California 93740. *Received March 25, 1985*

Abstract: The general base catalyzed addition of water to a series of triarylmethyl carbocations has been studied in aqueous solution with a series of substituted quinuclidines as base catalysts. Brønsted β values for general base catalysis range from 0.33 for trianisylmethyl carbocation, TAM (pK_{R^+} = 0.82), to 0.52 for Malachite Green, MG (pK_{R^+} = 6.94). There is a slight tendency for the β values to decrease with decreasing carbocation stability. The rate constants for the "water"-catalyzed reactions show a large positive deviation (800-fold in the case of Malachite Green) and the rate constants for the hydroxide ion catalyzed reactions a small negative deviation from Brønsted plots based on quinuclidine catalysis. These results are consistent with a concerted mechanism for the buffer-catalyzed reactions, a stepwise mechanism that proceeds through an oxonium ion intermediate for the "water"-catalyzed reactions (this mechanism corresponds to an A-1 mechanism in the microscopic reverse direction), and either a concerted or preassociation mechanism for the hydroxide ion catalyzed reactions. The positive deviation of water and the negative deviation of the hydroxide ion from the Brønsted relationship are opposite the deviations that are normally observed for these species in related reactions: compared to these related reactions, the pH range where buffer catalysis is strongest is shifted to higher pH values. These results also explain why the early attempts to find general base catalysis of the addition of water to triarylmethyl carbocations with acetate buffers proved unsuccessful.

There are two general-type mechanisms available for the reactions of alcohols to form carbocations: stepwise A-1 mechanisms that proceed through an intermediate (an oxonium ion) either free or associated with the catalyst[1] and a concerted mechanism which

0002-7863/85/1507-8218$01.50/0